remote sensing

MDPI

Editorial

Editorial for Special Issue "Earth Radiation Budget"

Steven Dewitte

Royal Meteorological Institute of Belgium, B-1180 Brussels, Belgium; steven.dewitte@meteo.be

Received: 18 August 2020; Accepted: 24 September 2020; Published: 16 October 2020

Abstract: The Earth Radiation Budget (ERB) at the top of the atmosphere describes how the Earth gains energy from the Sun and loses energy to space through the reflection of solar radiation and the emission of thermal radiation. The ERB is measured from space with dedicated remote sensing instruments. Its long-term monitoring is of fundamental importance for understanding climate change. This Special Issue contains contributions focusing on ERB remote sensing instruments for either (1) the establishment of past and current ERB Climate Data Records (CDRs), (2) insights in climate change gained from the analysis of ERB CDRs, and 3) the outlook for continued or improved future ERB monitoring.

Keywords: Earth Radiation Budget; Outgoing Longwave Radiation; Reflected Solar Radiation; Earth Energy Imbalance

---

1. Insights in Climate Change from Past and Current Earth Radiation Budget Climate Data Records

The ERB consists of separate terms, for which separate CDRs can be constructed:

- the Incoming Solar Radiation (ISR)—quantified through the Total Solar Irradiance (TSI)
- the Reflected Solar Radiation (RSR)
- the Outgoing Longwave Radiation (OLR)

1.1. Outgoing Longwave Radiation

Ref. [1] discusses CDRs of the OLR, obtained with the dedicated broadband Cloud's and the Earth's Radiant Energy System (CERES) instruments from 2000 to 2018, and with the High-resolution Infrared Radiation Sounder (HIRS) instruments from 1985 to 2018. During the period of overlap the Root Mean Square Difference (RMSD) between HIRS and CERES is 0.15 W/m^2, giving an indication of the stability by which the OLR can be monitored.

The primary cause of climate change is the increase of greenhouse gases, characterised by the greenhouse gas radiative forcing RF_{GHG}. The primary effect of those greenhouse gases is to decrease the OLR by $-\mathrm{RF}_{GHG}$. As a result the Earth Energy Imbalance (EEI), defined as EEI = ISR-RSR-OLR, becomes positive and the Earth's temperature rises. The temperature increase ΔT provokes secondary changes of the OLR, which in general are assumed to be linearly related to ΔT:

$$\Delta OLR = -RF_{GHG} + k_{LW} * \Delta T \tag{1}$$

k_{LW} is the longwave climate feedback parameter. From the available HIRS and CERES OLR CDRs, k_{LW} can be determined empirically by regressing OLR + RF_{GHG} as a function of ΔT. The determination of k_{LW} is illustrated in Figure 1. The results are summarised in Table 1.

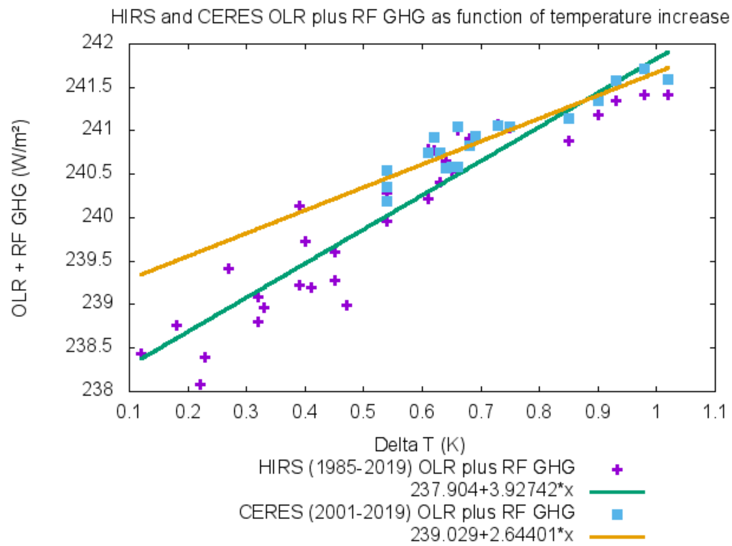

Figure 1. Outgoing Longwave Radiation plus greenhouse gas radiative forcing as a function of the Earth's temperature increase compared to pre-industrial conditions. Purple crosses: HIRS OLR measurements for the period 1985–2019. Green line: linear fit to HIRS OLR. Blue stars: CERES OLR measurements for the period 2001–2019. Orange line: linear fit to CERES OLR.

Table 1. Empirical determination of the longwave climate feedback parameter.

Instrument	Period	k_{LW}
HIRS	1985–2019	3.93 +/− 0.27 (1 σ) W/m^{2}K
CERES	2001–2019	2.64 +/− 0.24 (1 σ) W/m^{2}K

HIRS provides a longer time series then CERES. CERES can be expected to have a better stability then HIRS. The CERES based estimate of k_{LW} = 2.64 +/− 0.24 (1 σ) W/m^{2}K is comparable to climate model based estimates [2], while the HIRS based estimate of k_{LW} = 3.93 +/− 0.27 (1 σ) W/m^{2}K is not.

1.2. Reflected Solar Radiation

Ref. [3] discusses the CDR of the RSR, measured by the CERES instruments from 2000 to 2018. The 2000–2018 trend of the original CERES Energy Balanced and Filled (EBAF) RSR is −0.64 W/m^{2}dec. In [3] it is suggested that the CERES RSR measurements are subject to an instrumental drift of −0.5 %/dec. If this drift is removed, the drift corrected CERES RSR has a 2000–2018 trend of −0.14 W/m^{2}dec. When it is assumed equally likely that the suggested instrumental drift exists or not, the uncertainty interval for the 2000–2018 RSR trend is −0.39 +/− 0.25 W/m^{2}dec.

Elements which can explain systematic trends of the RSR are the melting of the Arctic sea ice, discussed in [3], and also long term changes of the surface albedo, of which an example is discussed in [4].

1.3. Incoming Solar Radiation

Following [3], the ISR has a 2000–2018 trend of −0.07 W/m^{2}dec. The downward trend is due to the lower amplitude of the solar activity cycle 24 (extending from 12/2008 to 05/2020) compared to the preceding solar activity cycle 23 (extending from 08/1996 to 12/2008).

The CERES EBAF ISR is based on the observations from the Total Irradiance Monitor (TIM) instrument [5] on the Solar radiation and Climate Explorer (SORCE) satellite. Following [6], the TIM/SORCE ISR has an instrumental drift of 0.09 W/m^{2}dec. Thus the CERES EBAF ISR 2000–2018 trend is 0.02 W/m^{2}dec.

1.4. Earth Energy Imbalance

Following [3], the 2000–2018 EEI trend is -0.16 W/m^{2}dec.

The CERES EBAF EEI 2000–2018 trend differs from the one found in [3], due to the assumed CERES RSR and TIM/SORCE ISR instrumental drifts. The 2000-2018 CERES EBAF EEI trend is 0.43 W/m^{2}dec.

When the 2000–2018 EEI trends from CERES EBAF and [3] are assumed equally likely, the combined uncertainty interval is 0.135 +/− 0.295 W/m^{2}dec. The most likely estimate of the EEI variations is then the mean of the two estimates, shown as the purple curve in Figure 2. The EEI has been normalised to a value of 0.9 W/m^2 over the period 2005–2014 following [7]—see purple curve in Figure 2.

An independent estimate of the EEI and its time variation can be obtained from the Ocean Heat Content Time Derivative (OHCTD). The green curve in Figure 2, obtained following a procedure similar to [3], shows the EEI estimated from the Ocean Heat Content (OHC) measurements cited in [8]. The corresponding 1975–2012 EEI trend is 0.142 +/− 0.015 W/m^{2}dec.

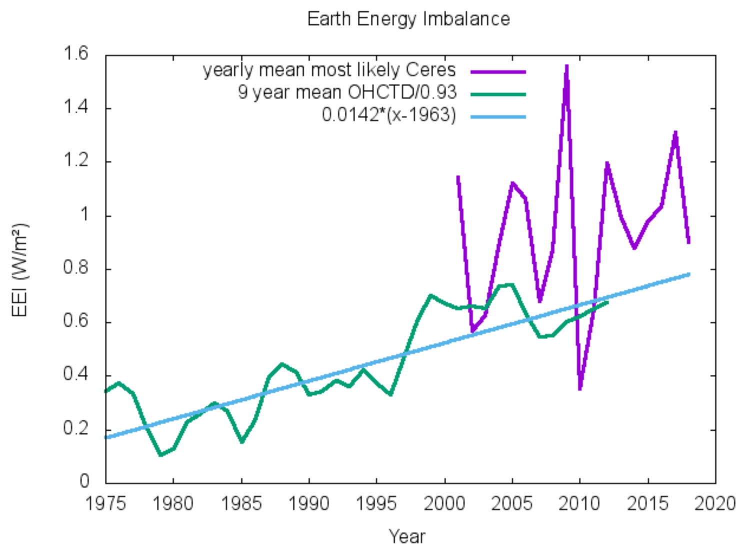

Figure 2. Comparison of independent estimates of EEI variations. Purple curve: most likely estimate of EEI from Ceres. Green curve: 9 year running mean EEI derived from OHCTD. Blue line: linear fit to green curve.

The new results presented in figure 2 can be considered as an update compared to [3]. For CERES, an increased uncertainty interval is obtained by considering the CERES EBAF and the interpretation of [3] as equally likely. For the OHCTD, more recent results are used from [8] compared to [9]. While in [3] a trend reversal of de EEI around 2000 was identified, now it appears more likely that over the entire period from 1975 to 2018, the EEI has increased with a more or less constant trend. The long term mean EEI trend can be estimated with the lowest uncertainty from the OHCTD as 0.142 +/− 0.015 W/m^{2}dec.

2. Outlook for Continued or Improved Future ERB Monitoring

For extension of the ERB record prior to the CERES period, the Advanced Very High Resolution Radiometer (AVHRR) is potentially useful. Ref. [10] discusses the reconstruction of the RSR from AVHRR, and [11] discusses the reconstruction of the OLR from AVHRR.

Ref. [12] presents the Radiometer Assessment using Vertically Aligned Nanotubes (RAVAN) cubesat—launched in 2016—which provides a low resolution wide field of view ERB measurement.

Ref. [13] describes the design of an accurate wide field of view ERB radiometer, to be combined with wide field of view imagers for increasing the resolution.

Ref. [14] presents calculations related to a possible future moon-based ERB observation.

3. Other Contributions

Ref. [15] presents an example of the regional analysis of the ERB.

Funding: This research received no external funding.

Conflicts of Interest: The author declares no conflict of interest.

References

1. Dewitte, S.; Clerbaux, N. Decadal Changes of Earth's Outgoing Longwave Radiation. *Remote Sens.* **2018**, *10*, 1539. [CrossRef]
2. Soden, B.; Held, I. An assessment of climate feedbacks in coupled ocean–atmosphere models. *J. Clim.* **2006**, *19*, 3354–3360. [CrossRef]
3. Dewitte, S.; Clerbaux, N.; Cornelis, J. Decadal Changes of the Reflected Solar Radiation and the Earth Energy Imbalance. *Remote Sens.* **2019**, *11*, 663. [CrossRef]
4. Tian, L.; Chen, J.; Shao, C. Interdependent Dynamics of LAI-Albedo across the Roofing Landscapes: Mongolian and Tibetan Plateaus. *Remote Sens.* **2018**, *10*, 1159. [CrossRef]
5. Kopp, G.; Lawrence, G. The total irradiance monitor (TIM): instrument design. *Sol. Phys.* **2005**, *230*, 91–109. [CrossRef]
6. Dewitte, S.; Nevens, S. The total solar irradiance climate data record. *Astrophys. J.* **2016**, *830*, 25. [CrossRef]
7. Trenberth, K.E.; Fasullo, J.T.; Von Schuckmann, K.; Cheng, L. Insights into Earth's energy imbalance from multiple sources. *J. Clim.* **2016**, *29*, 7495-7505. [CrossRef]
8. Cheng, L.; Zhu, J.; Abraham, J.; Trenberth, K.E.; Fasullo, J.T.; Zhang, B.; Yu, F.; Wan, L.; Chen, X.; Song, X. 2018 Continues Record Global Ocean Warming. *Adv. Atmos. Sci.* **2019**, *36*, 249–252. [CrossRef]
9. Cheng, L.; Trenberth, K.E.; Fasullo, J.; Boyer, T.; Abraham, J.; Zhu, J. Improved estimates of ocean heat content from 1960 to 2015. *Sci. Adv.* **2017**, *3*, e1601545. [CrossRef] [PubMed]
10. Akkermans, T.; Clerbaux, N. Narrowband-to-Broadband Conversions for Top-of-Atmosphere Reflectance from the Advanced Very High Resolution Radiometer (AVHRR). *Remote Sens.* **2020**, *12*, 305. [CrossRef]
11. Clerbaux, N.; Akkermans, T.; Baudrez, E.; Velazquez Blazquez, A.; Moutier, W.; Moreels, J.; Aebi, C. The Climate Monitoring SAF Outgoing Longwave Radiation from AVHRR. *Remote Sens.* **2020**, *12*, 929. [CrossRef]
12. Swartz, W.H.; Lorentz, S.R.; Papadakis, S.J.; Huang, P.M.; Smith, A.W.; Deglau, D.M.; Yu, Y.; Reilly, S.M.; Reilly, N.M.; Anderson, D.E. RAVAN: CubeSat Demonstration for Multi-Point Earth Radiation Budget Measurements. *Remote Sens.* **2019**, *11*, 796. [CrossRef] [PubMed]
13. Schifano, L.; Smeesters, L.; Geernaert, T.; Berghmans, F.; Dewitte, S. Design and Analysis of a Next-Generation Wide Field-of-View Earth Radiation Budget Radiometer. *Remote Sens.* **2020**, *12*, 425. [CrossRef]
14. Duan, W.; Huang, S.; Nie, C. Entrance Pupil Irradiance Estimating Model for a Moon-Based Earth Radiation Observatory Instrument. *Remote Sens.* **2019**, *11*, 583. [CrossRef]
15. Kim, B.-Y.; Lee, K.-T. Radiation Component Calculation and Energy Budget Analysis for the Korean Peninsula Region. *Remote Sens.* **2018**, *10*, 1147. [CrossRef]